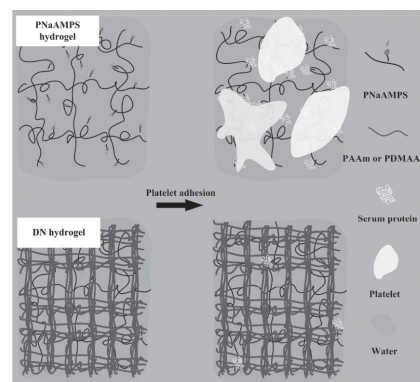


# In Vitro Platelet Adhesion of PNaAMPS/PAAm and PNaAMPS/PDMAAm Double-Network Hydrogels

Wen Jiang Zheng, Zhen Qi Liu, Feng Xu, Jie Gao, Yong Mei Chen,\*  
Jian Ping Gong, Yoshihito Osada

Nowadays, tough double-network (DN) hydrogels have attracted great attention owing to their excellent mechanical properties and good biocompatibility, which give them the potential to be used as blood-contacting soft tissue prostheses and medical devices. However, the study of platelet adhesion behavior on the surface of DN hydrogels has not been reported yet. In this work, the human platelet adhesion on the surface of poly (sodium 2-acrylamido-2-methyl-propanesulfonate) PNaAMPS/poly acrylamide (PAAm) and PNaAMPS/poly (*N,N'*-dimethylacrylamide) (PDMAAm) DN hydrogels is investigated under static conditions in vitro. The numbers of adherent platelets on PNaAMPS/PAAm and PNaAMPS/PDMAAm hydrogels are  $16 \pm 7$  and  $9 \pm 8$  cells per  $10^4 \mu\text{m}^2$ , respectively, which are far less than  $297 \pm 41$  cells per  $10^4 \mu\text{m}^2$  on polyethylene terephthalate (PET) and  $187 \pm 26$  cells per  $10^4 \mu\text{m}^2$  on negatively charged PNaAMPS (4 mol%) hydrogel. The results indicate the excellent antiplatelet performance of DN hydrogels. Moreover, the platelet adhesion mechanism is also discussed. The platelet adhesion is affected by the chemical component, zeta potential, and serum proteins adsorption of the hydrogel.



## 1. Introduction

Hydrogel is a kind of soft materials with large amount of water in their shape-retentive 3D network,<sup>[1,2]</sup> which has been widely used in biomedical fields,<sup>[3]</sup> such as tissue

engineering,<sup>[4]</sup> drug delivery,<sup>[5]</sup> medical device,<sup>[6]</sup> and biosensor.<sup>[7]</sup> However, because of the brittleness and fragility, traditional hydrogels are not competent to the applications requiring high mechanical performance. In the past decade, a series of tough hydrogels including

W. J. Zheng, Z. Q. Liu, Dr. J. Gao  
School of Science, State Key Laboratory for Mechanical Behavior of Materials, Collaborative Innovation Center of Suzhou Nano Science and Technology, Jiaotong University, Xi'an 710049, P.R. China  
Prof. F. Xu  
School of Life Science and Technology, MOE Key Laboratory of Biomedical Information Engineering, Xi'an Jiaotong University, Xi'an 710049, P.R. China  
Prof. F. Xu  
Bioinspired Engineering and Biomechanics Center, Xi'an Jiaotong University, Xi'an 710049, P.R. China

Prof. Y. M. Chen  
School of Science, State Key Laboratory for Mechanical Behavior of Materials, Collaborative Innovation Center of Suzhou Nano Science and Technology, Xi'an Jiaotong University, Xi'an 710049, P.R. China  
E-mail: chenym@mail.xjtu.edu.cn  
Prof. J. P. Gong  
Faculty of Advanced Life Science, Hokkaido University, Sapporo 060-0810, Japan  
Prof. Y. Osada  
RIKEN, Hirosawa, Wako, Saitama 351-0198, Japan

topological hydrogel,<sup>[8]</sup> nanocomposite hydrogel,<sup>[9,10]</sup> interpenetrating network,<sup>[11]</sup> and double-network (DN) hydrogel<sup>[12–18]</sup> has been developed. These tough hydrogels start a new application era of soft materials.

Among various tough hydrogels, DN hydrogels consist of two kinds of independent single network,<sup>[14]</sup> a brittle network plays as the sacrificial bonds and reduce stress concentration, and a soft, long-chain neutral network, poly acrylamide (PAAm) or poly (*N,N'*-dimethylacrylamide) (PDMAAm), serves as a role of bearing large deformation and stress. The mechanical properties of the DN hydrogels can be tuned by using different monomers or polymers, adjusting cross-linking concentrations and controlling gelation conditions. The mechanical performance of DN hydrogels can be tuned in a wide range, such as Young's modulus (0.1–1.0 MPa) and mechanical strength (failure compressive stress (20–60 MPa), failure compressive strain (90%–95%), failure tensile stress (1–10 MPa), and failure tensile strain (1000%–2000%), as well as tearing fracture energy (100–1000 J m<sup>2</sup>).<sup>[12]</sup> Besides the great mechanical performance, DN hydrogels also have a lot of superior properties, such as good biocompatibility,<sup>[19–22]</sup> excellent histocompatibility,<sup>[21,23]</sup> low sliding friction,<sup>[22,24]</sup> and excellent wear resistance.<sup>[22,25]</sup> Therefore, DN hydrogels have a great potential to be used as blood-contacting biomaterials (e.g., blood vessel, heart valve), as well as medical devices of minimally invasive interventions (catheter, stent). For those purpose, it is vital to study platelet adhesion of DN hydrogels, which however has not been explored yet.

The anionic sodium 2-acrylamido-2-methyl-propanesulfonate (NaAMPS) as well as the nonionic acrylamide (AAm) and *N,N'*-dimethylacrylamide (DMAAm) was chosen as the monomers for poly (sodium 2-acrylamido-2-methyl-propanesulfonate) (PNaAMPS/PAAm and PNaAMPS/PDMAAm DN hydrogels, respectively). In comparison with DN hydrogels, the mechanical properties of PAAm and PDMAAm are too weak for biomedical application. Thus, the DN hydrogels are the main object of platelet adhesion study. To understanding the platelet adhesion mechanism of PNaAMPS/PAAm and PNaAMPS/PDMAAm DN hydrogels, it is necessary to study the platelet adhesion behavior of their components, i.e., the neutral networks (PAAm and PDMAAm) and negatively charged network (PNaAMPS). The platelet adhesion of these two kinds of DN hydrogels as well as PNaAMPS, PAAm, and DMAAm hydrogel has been evaluated under static conditions in vitro. The platelet adhesion behavior of those hydrogels was evaluated in terms of the platelet number and morphology. The numbers of adherent platelet on PNaAMPS/PAAm and PNaAMPS/PDMAAm hydrogels were  $16 \pm 7$  and  $9 \pm 8$  cells per  $10^4 \mu\text{m}^2$ , respectively. They were far less than the number of adherent platelet on polyethylene terephthalate (PET)

( $297 \pm 41$  cells per  $10^4 \mu\text{m}^2$ ), which is a widely used blood-contacting biomaterial.<sup>[26–28]</sup> Through the further investigations of the platelet adhesion mechanism, we found that the chemical components, zeta potential, and protein adsorption were the main influence factors on hydrogels platelet adhesion behavior.

## 2. Experimental Section

### 2.1. Materials

Negatively charged monomer, i.e., 2-acrylamido-2-methyl-1-propanesulfonic acid sodium (NaAMPS) was prepared as previously reported.<sup>[29]</sup> Neutral monomers, i.e., *N,N'*-dimethylacrylamide (DMAAm) (Tokyo Kasei Kogyo, Tokyo, Japan) and acrylamide (AAm) (Junsei chemicals, Tokyo, Japan), as well as the initiator, 2-oxoglutaric acid (Wako Pure Chemicals, Osaka, Japan), and the cross-linking agent, *N,N'*-methylenebis-(acrylamide) (MBAA) (Tokyo Kasei Kogyo, Tokyo, Japan) were used as purchased.

### 2.2. Hydrogel Preparation

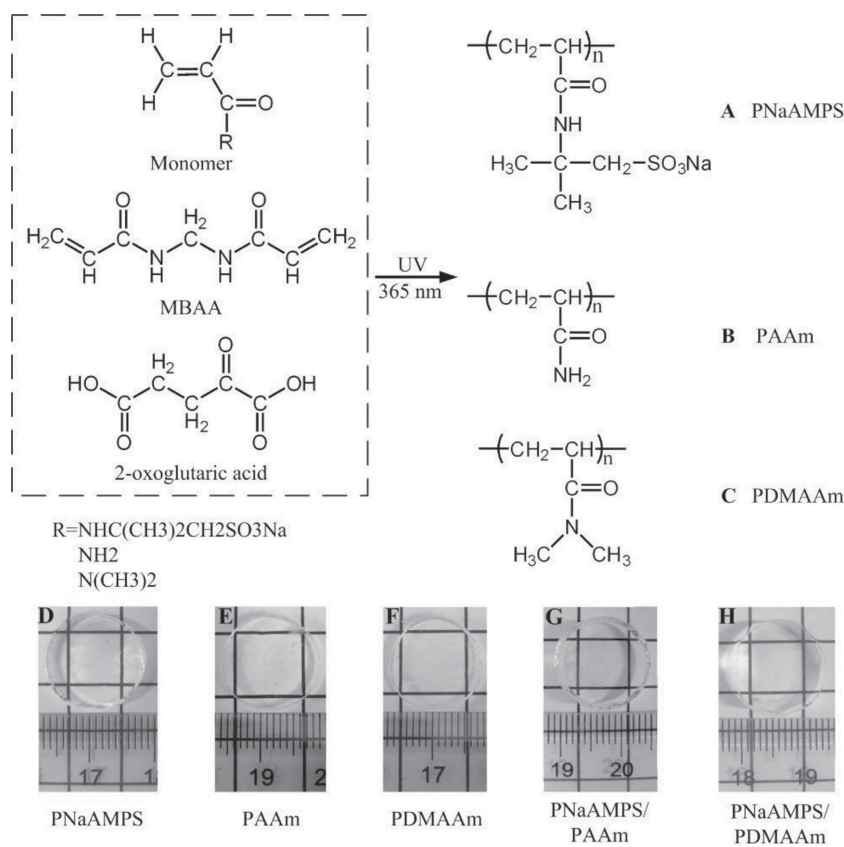
Sheet-shaped DN hydrogels, PNaAMPS/PDMAAm and PNaAMPS/PAAm, were synthesized by free radical polymerization.<sup>[12]</sup> Briefly, as-prepared 4 mol% PNaAMPS sheet was immersed in the monomer aqueous solution containing 3 mol L<sup>-1</sup> neutral monomer (DMAAm or AAm) and 0.1 mol% initiator (2-oxoglutaric acid) for 2 d at room temperature. The DN hydrogels were synthesized by UV irradiation (6 h) of the immersed PNaAMPS hydrogel, which had absorbed a large amount of neutral monomer in its polymer network. Single-network hydrogels of PNaAMPS, PAAm, and PDMAAm with different cross-linking concentration (the molar percent of cross-linker, MBAA, in relative to the monomer used in gelation) were also prepared as the control.<sup>[30]</sup> Then phosphate buffer solution (PBS)-equilibrated hydrogels were prepared by leaving the hydrogels in ion-exchanged water for 4 d and PBS for 3 d sequentially to extract residual chemicals that did not react during the gelation process. The chemical structure and photographs of the PBS-equilibrated single-network hydrogels and DN hydrogels are shown in Scheme 1.

### 2.3. Hydrogel Characterization

In order to evaluate the properties of hydrogel under physiological conditions (pH 7.4, ionic strength 0.15 M), all hydrogels used for characterizations were prepared by immersing PBS-equilibrated hydrogels in fetal bovine serum (FBS)-free culture medium (Medium 199, Sigma-Aldrich) for 24 h.<sup>[31]</sup> Before testing, the FBS-free hydrogels were sterilized by autoclaving (120 °C, 20 min).

#### 2.3.1. Swelling Degree

The swelling degree ( $q$ ) of hydrogels was quantified as the weight ratio of the swollen state ( $W_s$ ) of the hydrogel to that of the dry state ( $W_d$ ), i.e.,  $q = W_s/W_d$ . Each value was averaged over at least three parallel samples.



**Scheme 1.** Synthesis of double- (or single) network hydrogels. A) PNaAMPS hydrogel, B) PAAm hydrogel, C) PDMAAm hydrogels. The single-network hydrogels and DN hydrogels equilibrated in PBS and after high temperature sterilization were illustrated with photographs of D) PNaAMPS, E) PAAm, F) PDMAAm, G) PNaAMPS/PAAm, and H) PNaAMPS/PDMAAm hydrogels, respectively.

### 2.3.2. Mechanical Properties

The mechanical properties including Young's modulus ( $E$ ), fracture stress ( $\sigma$ ), and fracture strain ( $\lambda$ ) of hydrogels were tested by compressive stress–strain measurements using a tensile-compressive tester (CMT6503, MTS, USA). The hydrogel samples (15 mm diameter,  $\approx 2$  mm thickness) were compressed at a strain rate of  $10\% \text{ min}^{-1}$  at room temperature.  $E$  was determined by fitting the initial slopes of stress–strain curves in the range of 0.05 to 0.1 of strain ratio,<sup>[32]</sup> while  $\sigma$  and  $\lambda$  were determined as the stress and strain at the critical fracture points. Each value was averaged over 3–5 parallel samples.

### 2.3.3. Zeta Potential Measurement of Gels

The zeta potential ( $\zeta$ ) of single-network hydrogels was determined by using hydrogel particles.<sup>[29]</sup> Briefly, the electrophoretic mobility of the hydrogel particles ( $\approx 1 \mu\text{m}$  radius) dispersed in FBS-free medium was measured using Rank Mark II microelectrophoresis apparatus (Rank Brothers, Cambridge, England). The zeta potential was calculated using the Smoluchowski equation. For statistical purpose, the data for each hydrogel were recorded from 90 readings at least.

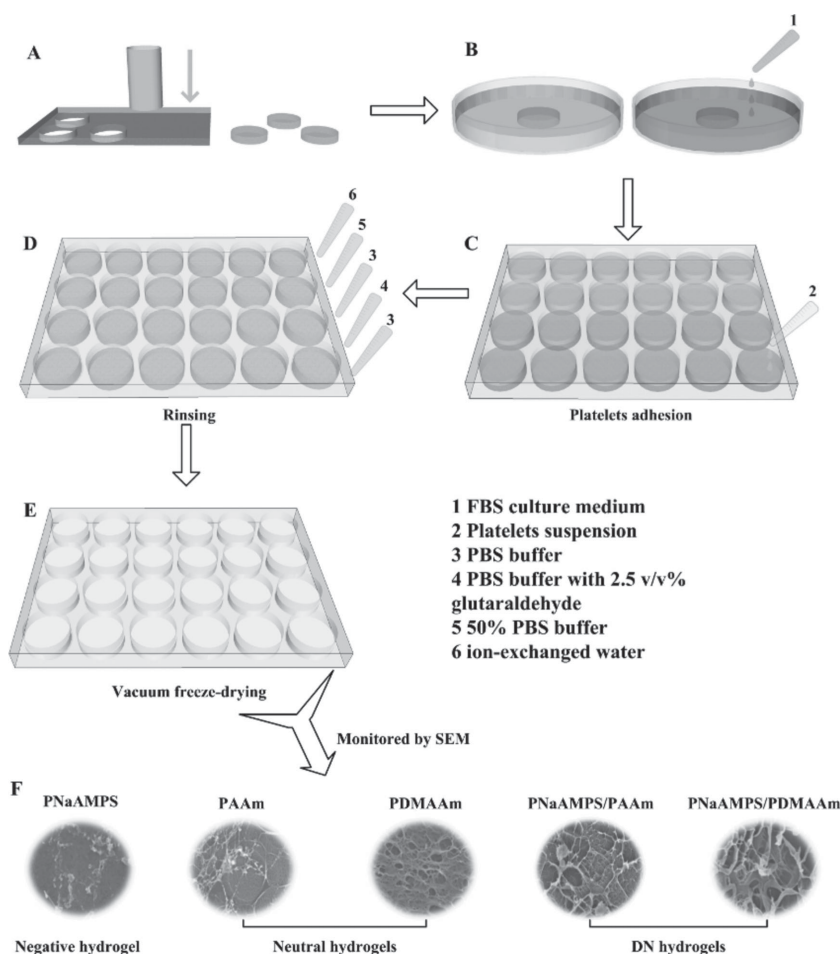
## 2.4. Platelet Adhesive Test

In order to check the effect of FBS on platelet adhesion, FBS-free hydrogels and FBS-equilibrated hydrogels (prepared by immersing sterilized FBS-free hydrogels in 1 mL 20% FBS (Invitrogen, Carlsbad, CA, USA) culture medium for 24 h) were used for platelet adhesive test. Human whole blood was donated from healthy volunteers and the procedure of platelet adhesive test in static conditions was the same as our previous studies.<sup>[29]</sup> Fresh blood obtained from healthy volunteers was mixed with a 3.8% sodium citrate solution in order to inhibit spontaneous coagulation (blood was collected following written informed consent from each volunteer in The Third Affiliated Hospital of Xi'an Jiaotong University with the help of professional staffs; the experimental use of human blood was approved by institutional ethics review boards). Platelet-rich plasma (PRP) and platelet-poor plasma (PPP) were obtained by centrifuging fresh blood at 1200 rpm for 5 min and 3500 rpm for 10 min at room temperature, respectively. PRP and PPP collection were performed within 2 h to avoid the change of properties of fresh blood. The platelet concentration was determined by hemocytometer under OLYMPUS IX 71 phase contrast microscope (Olympus, Tokyo, Japan) equipped with a digital camera using 20 $\times$  objective.  $1 \times 10^5$  cells  $\mu\text{L}^{-1}$  platelet suspension was prepared by mixing PRP and PPP. Then 200  $\mu\text{L}$  platelet suspension containing  $2 \times 10^7$  cells was dropped on each disk-shaped samples (15 mm in diameter), i.e., single-network

hydrogels and DN hydrogels, as well as PET used as a positive control. The platelet-loaded samples were incubated for 2 h at 37  $^\circ\text{C}$  in a humidified atmosphere of 5%  $\text{CO}_2$ . After rinsing off weakly adherent platelets on the sample surface by PBS (pH 7.4) for three times, the platelets adhered on the sample surface were fixed by 2.5 v/v% glutaraldehyde in PBS for 2 h at 37  $^\circ\text{C}$ . The fixed samples were further rinsed with PBS, 50% PBS and ion-exchanged water, respectively, to wash out glutaraldehyde and salts contained in PBS.

The morphology and number of adherent platelets were checked using scanning electron microscopy (SEM) (JEOL JSM-700P) after the secondary freeze-drying operation.<sup>[29]</sup> The dehydration process, which was automatically controlled by the temperature control program, was as follow: after the samples were frozen at  $-20 \text{ }^\circ\text{C}$  for 2 h in the chamber of vacuum freeze-drying oven (PowerDry LL1500, Thermo, USA), the frozen samples were subsequently dehydrated at  $-10 \text{ }^\circ\text{C}$  for 3 h and 25  $^\circ\text{C}$  for 4 h. The vacuum was higher than 100 mTorr during the freeze-drying run. The statistical density of adherent platelet was calculated from the number of adherent platelets on the representative area of the tested hydrogel surfaces (center point and the four symmetric points located  $\approx 5$  mm from the center point) over four independent experiments. Scheme 2





**Scheme 2.** Schematic representation of platelet adhesive test. A) Disk-shaped PBS-equilibrated hydrogels were punched out of the sheet-shaped hydrogels by a hole punch. B) The PBS-equilibrated hydrogels were sterilized by autoclaving (120 °C, 20 min) and then equilibrated in FBS-free and FBS containing medium for preparing FBS-free and FBS-equilibrated hydrogels, respectively. C) After the FBS-free hydrogels and FBS-equilibrated hydrogels were transferred into 24-well TCPS, platelet suspension was dropped onto the hydrogel surfaces, and the platelet-loaded samples were incubated for 2 h at 37 °C in a humidified atmosphere of 5% CO<sub>2</sub>. D) The platelets adhered on the sample surface were fixed by 2.5 v/v% glutaraldehyde after weakly adherent platelets were rinsed off by PBS (pH 7.4), and then the samples rinsed with PBS, 50% PBS, and ion-exchanged water, respectively. E) The hydrogel samples loaded with platelets is dehydrated. F) The dehydrated samples of three kinds of single-network hydrogels (PNaAMPS, PAAm, and PDMAAm) and two kinds of DN hydrogels (PNaAMPS/PAAm and PNaAMPS/PDMAAm) monitored by SEM.

shows the procedures of platelet adhesive test on the hydrogels in vitro.

## 2.5. Protein Adsorption of Hydrogels

To test the protein adsorption on the hydrogel surface, PBS-equilibrated hydrogel disks with a diameter of 2.5 cm were exposed to 1.67 mL of 20% FBS containing medium for 6 h to absorb the proteins in a 37 °C humidified atmosphere of 5% CO<sub>2</sub>. The loosely adsorbed proteins were washed out by ice-cold PBS. Then the adsorbed proteins were desorbed using 200 μL ice-cold lysis buffer (0.05 M Tris-HCl, 0.15 M NaCl, 0.001 M EDTA, and 0.5% Triton X-100) with fresh 1% protease inhibitor cocktail

(protease inhibitor cocktail set III, Calbiochem, La Jolla, CA) in the ice-bath. After the lysate was collected into a microfuge tube, all proteins contained in the lysate were measured by spectrophotometer at 595 nm according to the protocol of BSA Protein Assay Kit (Beyotime, China).

## 2.6. Statistical Analysis

All data were averaged over at least three parallel measurements and expressed as the form of mean ± standard deviation. The T-test was used for the valuation of statistical significance. It could be considered statistically significant when obtained \**P* < 0.05.

## 3. Results and Discussion

### 3.1. Hydrogel Characterization

Due to the excellent histocompatibility confirmed by our previous cell culture experiments and animal tests of subcutaneous and muscle implantation,<sup>[21,23]</sup> (PNaAMPS/PAAm) and PNaAMPS/PDMAAm DN hydrogels were chosen for the platelet adhesive test. The physicochemical properties including the water content and mechanical properties are important characters for hydrogels used as biomaterials.<sup>[33]</sup> The physical properties of hydrogels could be affected by high temperature during the sterilization process and the osmosis pressure from soaking in the saline solution. It is necessary to evaluate the physical properties of the hydrogels after sterilization and equilibration in PBS. It can be observed from photographs in Scheme 1, all the DN and single-network hydrogels keep transparent and homogeneous after

high temperature sterilizing. The degree of swelling (*q*), elastic modulus (*E*), fracture stress ( $\sigma$ ), and fracture strain ( $\lambda$ ) are shown in Table 1. In the case of same cross-linking concentration, *q* of anionic hydrogel was higher than that of nonionic hydrogel, which was due to the higher hydrophilicity of PNaAMPS compared to that of PAAm and poly(*N,N'*-dimethylacrylamide) (PDMAAm). In addition,  $\sigma$  and  $\lambda$  of PAAm and PDMAAm hydrogels were higher than PNaAMPS hydrogels because the soft and flexible polymer chains of PAAm and PDMAAm hydrogels can deform easily and be able to sustain higher external force than rigid PNaAMPS hydrogels. However, the single-network

**Table 1.** The degree of swelling ( $q$ ), elastic modulus ( $E$ ), fracture stress ( $\sigma$ ), and fracture strain ( $\lambda$ ) of FBS-free single-network hydrogels (PNaAMPS, PAAm, and PDMAAm), as well as FBS-free DN hydrogels (PNaAMPS/PAAm and PNaAMPS/PDMAAm).

Hydrogel	Cross-linking concentration [mol%]	$Q$	$E$ [MPa]	$\sigma$ [MPa]	$\lambda$ [%]
PNaAMPS	4	14.8 ± 0.36	0.048 ± 0.008	0.61 ± 0.04	42.3 ± 6.6
	10	9.4 ± 0.82	0.052 ± 0.005	0.63 ± 0.06	44.7 ± 4.7
PAAm	2	8.4 ± 1.35	0.088 ± 0.008	0.77 ± 0.04	80.6 ± 2.2
	4	7.2 ± 1.73	0.092 ± 0.006	0.74 ± 0.08	73.3 ± 5.8
PDMAAm	2	12.4 ± 0.17	0.063 ± 0.001	0.32 ± 0.05	44.1 ± 2.1
	4	9.68 ± 0.10	0.11 ± 0.008	0.41 ± 0.03	40.7 ± 5.8
PNaAMPS/PAAm	4/0.1	13.6 ± 2.66	0.16 ± 0.080	16.3 ± 5.5	92.3 ± 4.2
PNaAMPS/PDMAAm	4/0.1	11.9 ± 2.3	0.19 ± 0.080	11.4 ± 2.9	90.2 ± 3.4

hydrogels could only withstand  $\approx 10$  kPa external mechanical loading. On the other hand,  $\sigma$  of PNaAMPS/PAAm and PNaAMPS/PDMAAm DN hydrogels was  $16.3 \pm 5.5$  and  $11.4 \pm 2.9$  MPa, respectively, which were about ten times higher than that of single-network hydrogels (Figure S1, Supporting Information). Moreover,  $\lambda$  of PNaAMPS/PAAm and PNaAMPS/PDMAAm DN hydrogels was  $\approx 90\%$ , which was obviously higher than that of single-network hydrogels. The mechanical strength of the DN hydrogels was high enough to be used as artificial blood-contacting biomaterials. These results demonstrate that PNaAMPS/PDMAAm and PNaAMPS/PAAm DN hydrogels are able to maintain their high mechanical properties even when they are sterilized under high temperature and immersed in the saline solution.

### 3.2. Platelet Adhesion on Hydrogels

The level of platelet activation can be assessed by their morphology.<sup>[34]</sup> Evaluating platelet activation through SEM observation is an effective approach, because SEM images can provide detailed morphology information of adherent platelets.<sup>[29,35,36]</sup> The samples used for SEM observation must be dried by the secondary freeze-drying operation, which is a very efficient method to avoid the shape distortion of platelets during drying.<sup>[29]</sup> The morphology of platelets monitored by SEM images can be classified into round, discoid, dendritic, and spread shape. Normally, nonactivated round platelets are spherical cells with average cell diameter of  $\approx 1\text{--}2$   $\mu\text{m}$ , thickness of  $\approx 1$   $\mu\text{m}$ . Discoid platelets are mildly flattened, absent of pseudopodia. Dendritic platelets are discoid cells with radiant fiber-like pseudopodia. Spread platelets are flat cells without pseudopodia, which can easily induce a second layer of platelets on the substrate-bound cells. The level of platelet activation is in the order of round platelet (nonactivated platelet) < discoid platelets (mildly activated platelet) < dendritic platelet (moderately activated platelet) < spread platelet (activated platelet).<sup>[34]</sup>

It has been proved that serum proteins contained in the FBS can affect platelet adhesion of samples.<sup>[35,37]</sup> Therefore, the platelet adhesion behaviors of the FBS-equilibrated hydrogels including the PNaAMPS/PAAm, PNaAMPS/PDMAAm DN hydrogels and PNaAMPS, PAAm, PDMAAm single-network hydrogels have been studied. The FBS-free hydrogels as control have also been tested to verify the effect of serum proteins on proteins adhesion behavior. There was only a few round platelets adhered on the surface of PNaAMPS/PAAm (Figure 1A–D) and PNaAMPS/PDMAAm (Figure 1 E–H) DN hydrogels. The number of platelets adhered on the surface of FBS-free PNaAMPS/PAAm and PNaAMPS/PDMAAm DN hydrogels was  $6 \pm 2$  and  $8 \pm 3$  cells per  $10^4$   $\mu\text{m}^2$ , respectively. Meanwhile, the number of platelets adhered on the surface of FBS-equilibrated PNaAMPS/PAAm and PNaAMPS/PDMAAm DN hydrogels was  $16 \pm 7$  and  $9 \pm 8$  cells per  $10^4$   $\mu\text{m}^2$ , respectively. Moreover, the adherent platelets are round shape, which means they were nonactivated. As a widely used blood-contacting biomaterial,<sup>[26–28]</sup> the platelet adhesion of PET has also been tested. The adherent platelets on PET surface were  $297 \pm 41$  cells per  $10^4$   $\mu\text{m}^2$  (Figure S2, Supporting Information). Compared with PET, the DN hydrogels have notable advantage in antiplatelet performance.

As an important constituent part of DN hydrogels, the platelet adhesion behavior of PNaAMPS was totally different from DN hydrogels. The presence of FBS can obviously change the platelet adhesion behavior of PNaAMPS hydrogels. Only a few round platelets adhered on the surface of 4 mol% ( $3 \pm 2$  cells per  $10^4$   $\mu\text{m}^2$ ) (Figure 2A,B) and 10 mol% ( $8 \pm 4$  cells per  $10^4$   $\mu\text{m}^2$ ) (Figure 2C,D) FBS-free PNaAMPS hydrogels. The strong electrostatic repulsion between negatively charged hydrogels and platelets causes the antiplatelet properties of FBS-free PNaAMPS.<sup>[29]</sup> However, the adherent platelets increased sharply on the surface of FBS-equilibrated PNaAMPS hydrogels. The number of round adherent platelets was  $187 \pm 26$

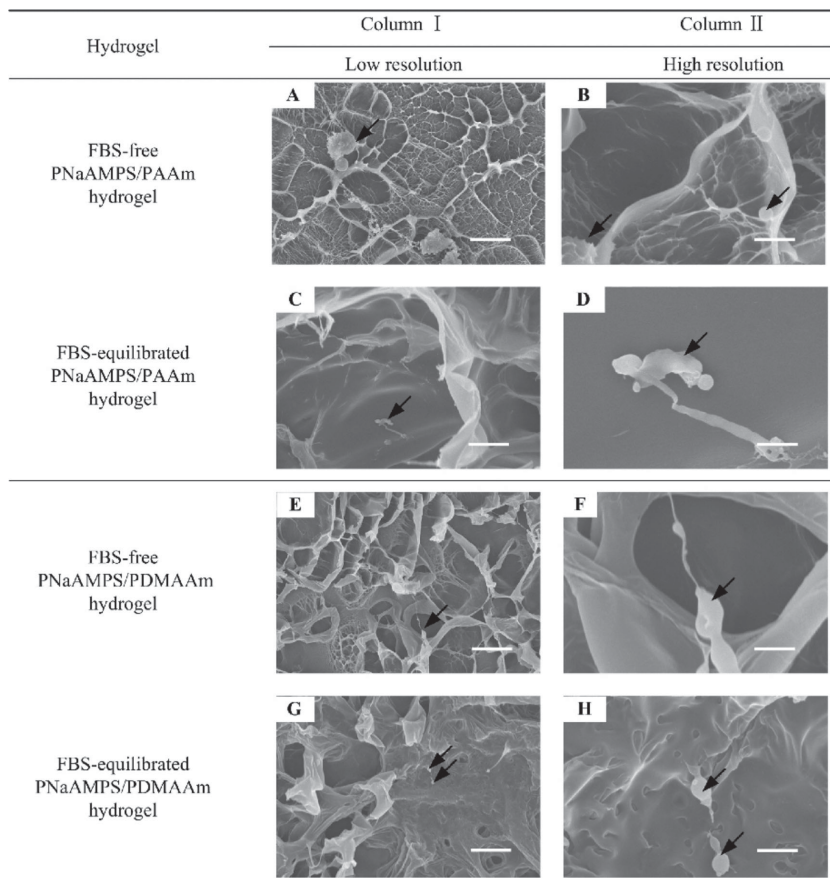


**Figure 1.** The SEM images of adherent platelets on FBS-free (A, B) and FBS-equilibrated (C, D) PNaAMPS/PAAm DN hydrogels, as well as on FBS-free (E, F) and FBS-equilibrated (G, H) PNaAMPS/PDMAAm DN hydrogels. Only a few round platelets adhered on the hydrogels, indicating nonactivation. Column II (scale bar: 5  $\mu\text{m}$ ) is the magnified images of Column I (scale bar: 50  $\mu\text{m}$ ), the adhered platelets are labeled by arrow.

(Figure 2 E,F) and  $197 \pm 30$  cells per  $10^4 \mu\text{m}^2$  (Figure 2 G,H) when cross-linking concentration was 4 mol% and 10 mol%, respectively. Moreover, a lot of discoid-shaped platelets and focal clumps were observed on the surface of FBS-equilibrated PNaAMPS hydrogels, the number of discoid-shaped platelets was  $143 \pm 32$  and  $151 \pm 40$  cells per  $10^4 \mu\text{m}^2$  when cross-linking concentration was 4 mol% and 10 mol%, respectively. The number of adherent platelets under FBS condition is  $\approx 27$  times of FBS-free condition. It has been reported that positively charged hydrogels can induce platelet adhesion because of the electronic attraction between the negatively charged platelets and the positively charged hydrogels.<sup>[38]</sup> The result here proves that the negatively charged hydrogels also induce platelet adhesion under the FBS condition. We speculated that serum proteins contained in FBS is the key factor for the platelet adhesion of FBS-equilibrated PNaAMPS.

We have also studied the platelet adhesion behavior of the nonionic PAAm and PDMAAm hydrogels, which constitute the second network of DN hydrogels. There is no

platelet found on the surface of PAAm (Figure S3, Supporting Information) and PDMAAm (Figure S4, Supporting Information) hydrogels. They showed an excellent antiplatelet performance whether pre-equilibrated in FBS or not. We speculated that the surface of these nonionic hydrogels does not induce the serum proteins adsorption. The similarity of antiplatelet performance between PNaAMPS/PAAm (PNaAMPS/PDMAAm) DN hydrogels and PAAm (PDMAAm) indicates the nonionic PAAm and PDMAAm network dominate the surface properties of DN hydrogels.

In addition, it was found that the cross-linking concentration of PNaAMPS, PAAm, and PDMAAm hydrogels does not affect the platelet adhesion behavior (Figure 3). The cross-linking concentration can influence the mechanical performance of hydrogels directly. This result indicates that the change of mechanical properties does not affect the platelet adhesion behavior of the hydrogels. The DN hydrogels can fulfill the various mechanical requirements in the application and keep an excellent antiplatelet performance.

To sum up, platelets do not adhere to the surface of all those hydrogels without the FBS. The antiplatelet performance of FBS-equilibrated hydrogels is in the order of PNaAMPS/

PAAm  $\approx$  PNaAMPS/PDMAAm  $\approx$  PAAm  $\approx$  PDMAAm  $>$  PNaAMPS. The PNaAMPS/PAAm and PNaAMPS/PDMAAm DN hydrogels as well as the neutral PAAm and PDMAAm hydrogels showed excellent antiplatelet performance. The platelet adhesion of FBS-equilibrated PNaAMPS hydrogel may be caused by the adsorption of serum proteins in FBS. The cross-linking concentration of hydrogels does not affect the platelet adhesion behavior of hydrogels. Consequently, the change of mechanical properties of hydrogels will not affect the platelet adhesion behavior of hydrogels.

### 3.3. Zeta Potential of Hydrogels and Protein Adsorption

When blood is applied to biomaterials, the proteins contained in blood will be absorbed on materials surface prior to cellular interaction with surface, and then the adsorbed proteins will promote platelet adhesion and activation, and result in thrombus at last.<sup>[39,40]</sup> So it is very important to understand the effect of protein adsorption on platelet



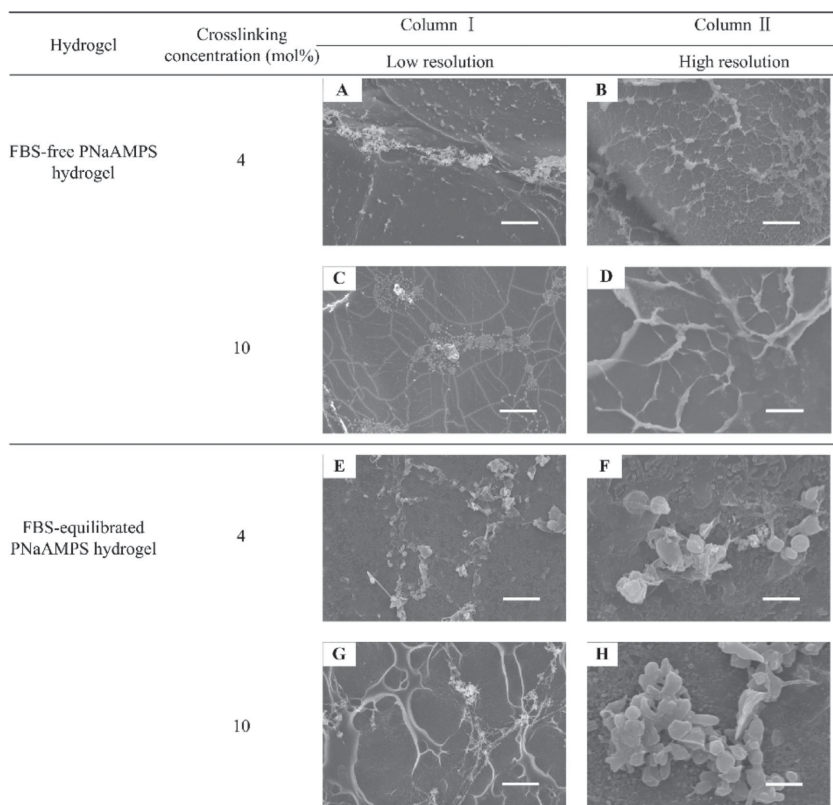


**Figure 2.** The SEM images of adherent platelets on FBS-free (A–D) and FBS-equilibrated (E–H) PNaAMPS hydrogels with 4 mol% and 10 mol% cross-linking concentration. A few round platelets adhered on FBS-free hydrogels, indicating nonactivation, while discoid-shaped platelets adhered on FBS-equilibrated hydrogels and form aggregates, indicating activation. Column II (scale bar: 5  $\mu\text{m}$ ) is the magnified images of Column I (scale bar: 50  $\mu\text{m}$ ).

adhesion and activation. It was evidenced that platelet adhesion is closely related to the serum proteins (e.g., vitronectin, fibronectin, etc.). These serum proteins could be anchored on the surface of biomaterials via electrostatic interactions or van der Waals' force, and the adsorbed proteins can further affect the behavior of platelet adhesion.<sup>[41]</sup> In our investigation, we speculated that the serum proteins contained in FBS were adsorbed on the surface of FBS-equilibrated hydrogels before platelet adhesion, and these proteins may facilitate platelet adhesion and activation by providing more available binding sites for platelets. In addition, protein adsorption is closely related to zeta potential of hydrogels,<sup>[32,42]</sup> thus the zeta potential of hydrogels was measured to verify the speculation.

A series of poly (NaAMPS-*co*-DMAAm) hydrogels was synthesized to study the effect of charge on platelet adhesion and activation. The zeta potential of hydrogels can be tuned by changing the molar fraction of NaAMPS in the poly (NaAMPS-*co*-DMAAm) hydrogels. Then, platelet adhesion and activation under FBS condition were tested. The number of adherent platelets and SEM images is shown in Figure S5 and S6 (Supporting Information). The

zeta potential ( $\zeta$ ) decreases with the increasing of NaAMPS molar fraction.<sup>[42]</sup> The number of adherent platelets almost remains unchanged when the NaAMPS molar fraction  $\leq 0.3$ . Then a dramatic increasing occurs with the increasing of NaAMPS molar fraction from 0.3 to 0.7, the number of adherent platelets increases from  $21 \pm 9$  to  $187 \pm 126$  cells per  $10^4 \mu\text{m}^2$ . The number of adherent platelets almost keeps stable when NaAMPS molar fraction  $\geq 0.7$  (the number of adherent platelets is  $187 \pm 26$  and  $197 \pm 30$  cells per  $10^4 \mu\text{m}^2$  on PNaAMPS hydrogel with cross-linking concentration of 4 mol% and 10 mol%, respectively). This variation trend of platelet adhesion is similar with the serum protein adsorption on the poly (NaAMPS-*co*-DMAAm) hydrogels we previously reported.<sup>[42]</sup> That means the platelet adhesion on material surface is facilitated by the adsorption of serum protein. Meanwhile, from the SEM images of adherent platelets, discoid platelets were found on the poly (NaAMPS-*co*-DMAAm) hydrogel with a NaAMPS molar fraction of 0.7 (Figure S6D, Supporting Information). Those results indicate that more negative charge, more protein adsorption, which favors platelet adhesion and activation.

Figure 4A shows the zeta potential of DN and single-network hydrogels. The value of zeta potential of each hydrogel is in the order of PAAm>PDMAAm>PNaAMPS/PAAm>PNaAMPS/PDMAAm>>PNaAMPS. The zeta potential of the DN hydrogels was lower than that of neutral PAAm and PDMAAm hydrogels because of the existence of anionic PNaAMPS component in the DN hydrogels. While, the zeta potential of PNaAMPS was far lower than DN hydrogel. The similarity of zeta potential between DN hydrogels and PAAm, PDMAAm hydrogels indicates that the surface property of DN hydrogels is dominated by neutral polymer network. This is in good agreement with the previous results.

The amount of total adsorbed proteins on each hydrogel has a similar trend as the zeta potential (Figure 4B). The amount of total proteins adsorbed on anionic PNaAMPS hydrogels with the lowest zeta potential was noticeably higher than that of DN hydrogels and neutral PAAm and PDMAAm hydrogels. Because the proteins adsorbed on the hydrogel surface could facilitate platelet adsorption, a large number of platelets adhered on the FBS-equilibrated PNaAMPS hydrogels (Figure 3). The number of platelets

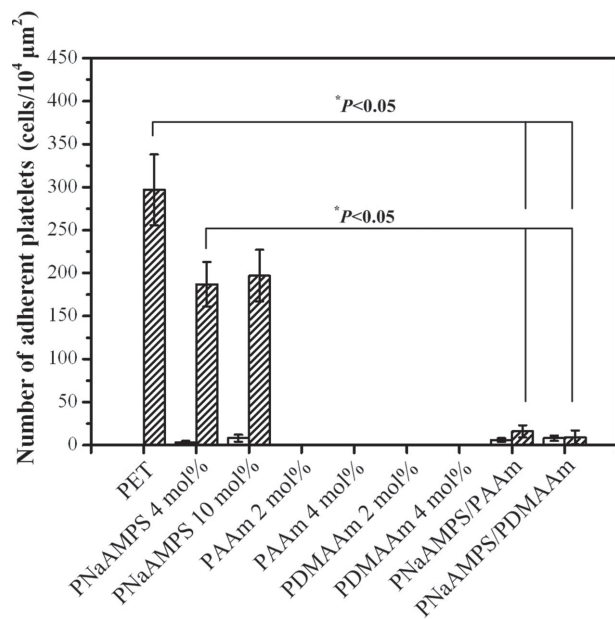


**Figure 3.** Number of adherent platelets on the surface of various FBS-free (white bar) and FBS-equilibrated hydrogels (white bar with oblique lines). The numbers with unit in mol% are the cross-linking concentration in molar ratio in relative to monomer used in gelation. \* $p < 0.05$  vs the FBS-equilibrated PNaAMPS hydrogels. Error ranges are standard deviations over  $n = 5$  samples.

adhered on the surface of DN hydrogels was much less than that of PNaAMPS hydrogels, which may be attributed to the fact that the surface properties of DN hydrogels are dominated by the neutral components, i.e., PAAm and PDMAAm, specifically due to the following two reasons: i) a large amount of PAAm or PDMAAm inevitably polymerized on the surface of DN hydrogels in the process of DN hydrogel preparation; ii) The molar ratios of neutral polymers, PAAm or PDMAAm, are over 10 times higher than that of negatively charged polymers in the DN

hydrogels.<sup>[14,15]</sup> The current work indicates that the surface properties and the behavior of platelet adhesion are mainly controlled by the neutral polymer network in DN hydrogels. Similar results were obtained in our previous endothelial cell cultivation.<sup>[42]</sup> The results demonstrate that the adsorbed proteins on the surface of hydrogels, which are directly related to the zeta potential of the hydrogel surface, play an important role in inducing platelet adhesion.

#### 4. Conclusion

DN hydrogels are promising blood-contacting biomaterials because their mechanical properties are comparable to that of native biological tissues. The static platelet adhesive test of two typical DN hydrogels, i.e., PNaAMPS/PAAm and PNaAMPS/PDMAAm, has been undertaken for the first time. These two DN hydrogels showed an excellent antiplatelet performance with or without the presence of the FBS. Only a few nonactivated round platelets adhered on DN hydrogels surface. There are  $6 \pm 2$  and  $8 \pm 3$  cells per  $10^4 \mu\text{m}^2$  on FBS-free PNaAMPS/PAAm and PNaAMPS/PDMAAm hydrogels. On FBS-equilibrated PNaAMPS/PAAm and PNaAMPS/PDMAAm hydrogels, the adhered platelets are  $16 \pm 7$  and  $9 \pm 8$  cells per  $10^4 \mu\text{m}^2$ , respectively. The adhesion and activation of platelets mainly depend on the chemical structure, zeta potential, and protein adsorption of the hydrogels surface. With the presence of serum proteins, the PNaAMPS (4 mol%) hydrogel with the lowest zeta potential of  $31.1 \pm 1.5$  mV adsorbed over three times weight of the proteins than that of DN hydrogels, and adsorbed over 10 times of platelets compared to that of platelets on DN hydrogels. Among these,  $143 \pm 32$  cells per  $10^4 \mu\text{m}^2$  of platelets were found active on the surface of PNaAMPS hydrogel. However, the nonionic PAAm and PDMAAm hydrogels, which are also the main components

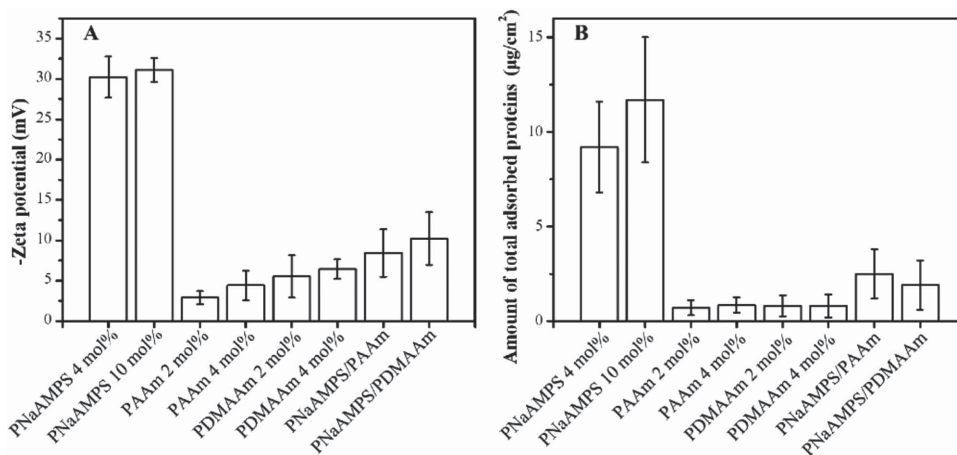


**Figure 4.** The zeta potential (A) and amount of total adsorbed proteins (B) of various hydrogels. The numbers with unit in mol% are the cross-linking concentration in molar ratio in relative to monomer used in gelation. Error ranges are standard deviations over  $n = 5$  samples.



of the DN hydrogels, present excellent antiplatelet performance. The antiplatelet performance of the DN hydrogels is dominated by the nonionic PAAm and PDMAAm network. Meanwhile, the cross-linking concentration does not affect the platelet adhesion behavior of hydrogels. As a result, DN hydrogels can maintain their excellent antiplatelet performance despite the tuning of mechanical properties, and this characteristic offers them great potential for using as blood-contacting biomaterials.

## Supporting Information

Supporting Information is available from the Wiley Online Library or from the author.

**Acknowledgements:** This research was supported by the National Natural Science Foundation of China (Grant 51173144, 51073127), International Science & Technology Cooperation Program supported by Ministry of Science and Technology of China and Shaanxi Province (2013KW14-02), the Research Fund for the Doctoral Program of Higher Education of China, the Scientific Research Foundation for the Returned Overseas Chinese Scholars, State Education Ministry, the Fundamental Research Funds for the Central Universities, the Program for Key Science and Technology Innovative Team of Shaanxi Province (No. 2013KCT-05), and Suzhou Research Institute (BY2013036). FX. was financially supported by the National Natural Science Foundation of China (11372243) and International Science & Technology Cooperation Program of China (2013DFG02930). The authors also thank the Third Affiliated Hospital of Xi'an Jiaotong University and all the volunteers for their help with blood collection.

Received: September 15, 2014; Revised: November 8, 2014; Published online: January 23, 2015; DOI: 10.1002/macp.201400481

**Keywords:** platelet adhesion; doublenetwork; hydrogel; platelet compatibility

- [1] E. S. Place, J. H. George, C. K. Williams, M. M. Stevens, *Chem. Soc. Rev.* **2009**, *38*, 1139.
- [2] Z. Li, Z. Wei, F. Xu, Y. H. Li, T. J. Lu, Y. M. Chen, G. J. Zhou, *Macromol. Rapid. Commun.* **2012**, *33*, 1191.
- [3] Z. Wei, J. H. Yang, X. J. Du, F. Xu, M. Zrinyi, Y. Osada, F. Li, Y. M. Chen, *Macromol. Rapid. Commun.* **2013**, *34*, 1464.
- [4] S. V. Vlierberghe, P. Dubruel, E. Schacht, *Biomacromolecules* **2011**, *12*, 1387.
- [5] Y. Qiu, K. Park, *Adv. Drug. Delivery Rev.* **2012**, *64*, 49.
- [6] K. Deligkaris, T. S. Tadele, W. Olthuis, A. V. D. Berg, *Sens. Actuators B Chem.* **2010**, *147*, 765.
- [7] H. Shibata, Y. J. Heo, T. Okitsu, Y. Matsunaga, T. Kawanishi, S. Takeuchi, *Proc. Natl. Acad. Sci. USA*, **2010**, *107*, 17894.
- [8] Y. Okumura, K. Ito, *Adv. Mater.* **2001**, *13*, 485.
- [9] K. Haraguchi, T. Takehisa, *Adv. Mater.* **2002**, *14*, 1120.
- [10] K. Haraguchi, R. Farnworth, A. Ohbayashi, T. Takehisa, *Macromolecules* **2003**, *36*, 5732.
- [11] J. Y. Sun, X. H. Zhao, W. R. K. Illeperuma, O. Chaudhuri, K. H. Oh, D. J. Mooney, J. J. Vlassak, Z. G. Suo, *Nature* **2012**, *489*, 133.
- [12] J. P. Gong, Y. Katsuyama, T. Kurokawa, Y. Osada, *Adv. Mater.* **2003**, *15*, 1155.
- [13] J. P. Gong, *Soft Matter* **2010**, *6*, 2583.
- [14] T. Nakajima, H. Furukawa, Y. Tanaka, T. Kurokawa, Y. Osada, J. P. Gong, *Macromolecules* **2009**, *42*, 2184.
- [15] Y. H. Na, T. Kurokawa, Y. Katsuyama, H. Tsukeshiba, J. P. Gong, Y. Osada, S. Okabe, T. Karino, M. Shibayama, *Macromolecules* **2004**, *37*, 5370.
- [16] Y. Tanaka, R. Kuwabara, Y. H. Na, T. Kurokawa, J. P. Gong, Y. Osada, *J. Phys. Chem. B* **2005**, *109*, 11559.
- [17] H. Tsukeshiba, M. Huang, Y. H. Na, T. Kurokawa, R. Kuwabara, Y. Tanaka, H. Furukawa, Y. Osada, J. P. Gong, *J. Phys. Chem. B* **2005**, *109*, 16304.
- [18] T. Kurokawa, H. Furukawa, W. Wang, Y. Tanaka, J. P. Gong, *Acta Biomater.* **2010**, *6*, 1353.
- [19] M. A. Haque, T. Kurokawa, J. P. Gong, *Polymer* **2012**, *53*, 1805.
- [20] T. Kurokawa, H. Furukawa, W. Wang, Y. Tanaka, J. P. Gong, *Acta Biomater.* **2010**, *6*, 1353.
- [21] Y. Tanabe, K. Yasuda, C. Azuma, H. Taniguro, S. Onodera, A. Suzuki, Y. M. Chen, J. P. Gong, Y. Osada, *J. Mater. Sci. Mater. Med.* **2008**, *19*, 1379.
- [22] Y. M. Chen, K. Dong, Z. Q. Liu, F. Xu, *Sci. China Technol. Sci.* **2012**, *55*, 2241.
- [23] C. Azuma, K. Yasuda, Y. Tanabe, H. Taniguro, F. Kanaya, A. Nakayama, Y. M. Chen, J. P. Gong, Y. Osada, *J. Biomed. Mater. Res. A* **2007**, *81*, 373.
- [24] D. Kaneko, T. Tada, T. Kurokawa, J. P. Gong, Y. Osada, *Adv. Mater.* **2005**, *17*, 535.
- [25] K. Yasuda, J. P. Gong, Y. Katsuyama, A. Nakayama, Y. Tanabe, E. Kondo, M. Ueno, Y. Osada, *Biomaterials* **2005**, *26*, 4468.
- [26] M. J. Moreno, A. Ajji, D. M. Kalhori, M. Rukhlova, A. Hadjizadeh, M. N. Bureau, *J. Biomed. Mater. Res. B* **2011**, *97*, 201.
- [27] R. A. Hoshi, R. V. Lith, M. C. Jen, J. B. Allen, K. A. Lapidis, G. Ameer, *Biomaterials* **2013**, *34*, 30.
- [28] D. Pankajakshan, V. K. Krishnan, L. K. Krishnan, *Biofabrication* **2010**, *2*, 041001.
- [29] Y. M. Chen, M. Tanaka, J. P. Gong, K. Yasuda, S. Yamamoto, M. Shimomura, Y. Osada, *Biomaterials* **2007**, *28*, 1752.
- [30] Y. M. Chen, N. Shiraishi, H. Satokawa, A. Kakugo, T. Narita, J. P. Gong, Y. Osada, K. Yamamoto, J. Ando, *Biomaterials* **2005**, *28*, 4588.
- [31] K. Y. Asuda, N. Kitamura, J. P. Gong, K. Arakaki, H. J. Kwon, S. Onodera, Y. M. Chen, T. Kurokawa, F. Kanaya, Y. Ohmiya, Y. Osada, *Macromol. Biosci.* **2009**, *9*, 307.
- [32] Y. M. Chen, R. Ogawa, A. Kakugo, Y. Osada, J. P. Gong, *Soft-Matter* **2009**, *5*, 1804.
- [33] Y. M. Chen, Z. Q. Liu, Z. H. Feng, F. Xu, J. K. Liu, *J. Biomed. Mater. Res., Part A* **2013**, *102*, 2258.
- [34] F. Jung, S. Braune, A. Lendlein, *Clin. Hemorheol. Microcirc.* **2013**, *53*, 97.
- [35] M. Tanaka, T. Motomura, M. Kawada, T. Anzai, Y. Kasori, T. Shiroya, K. Shimura, M. Onishi, A. Mochizuki, *Biomaterials* **2000**, *21*, 1471.
- [36] B. Sivaraman, R. A. Latour, *Biomaterials* **2010**, *31*, 832.
- [37] A. Higuchi, K. Sugiyama, B. O. Yoon, M. Sakurai, M. Hara, M. Sumita, S. Sugawara, T. Shirai, *Biomaterials* **2003**, *24*, 3235.
- [38] J. H. Lee, G. K. Hang, J. W. Lee, H. B. Lee, *J. Biomed. Mater. Res. A* **1998**, *40*, 180.
- [39] J. H. Lee, Y. M. Ju, D. M. Kim, *Biomaterials* **2000**, *21*, 683.
- [40] L. Cao, M. Chang, C. Lee, D. G. Castner, S. Sukavaneshvar, B. D. Ratner, T. A. Horbett, *J. Biomed. Mater. Res. A* **2007**, *81*, 827.
- [41] J. H. Lee, H. B. Lee, *J. Biomed. Mater. Res. A* **1998**, *41*, 304.
- [42] Y. M. Chen, J. P. Gong, M. Tanaka, K. Yasuda, S. Yamamoto, M. Shimomura, Y. Osada, *J. Biomed. Mater. Res. A* **2009**, *88*, 74.